Article

Reaction Dynamics of Phenyl Radicals in Extreme Environments: A Crossed Molecular Beam Study

Xibin Gu, and Ralf I. Kaiser

Acc. Chem. Res., **2009**, 42 (2), 290-302• DOI: 10.1021/ar8001365 • Publication Date (Web): 03 December 2008

ACCOUNTS
of chemical research

Reaction Dynamics of Phenyl Radicals in Extreme Environments: A Crossed Molecular Beam Study

XIBIN GU AND RALF I. KAISER*
Department of Chemistry, University of Hawaii at Manoa, Honolulu, Hawaii 96822

RECEIVED ON JUNE 5, 2008

CONSPECTUS

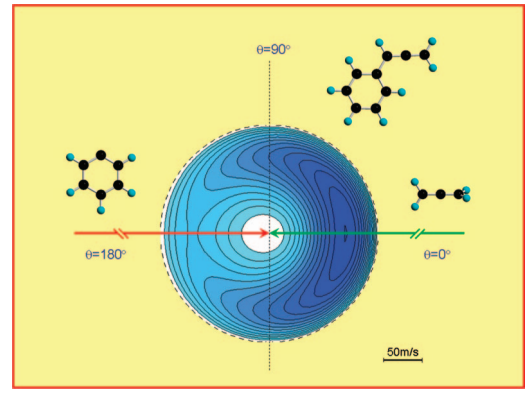

Polycyclic aromatic hydrocarbons (PAHs)—organic compounds that consist of fused benzene rings—and their hydrogen-deficient precursors have attracted extensive interest from combustion scientists, organic chemists, astronomers, and planetary scientists. On Earth, PAHs are toxic combustion products and a source of air pollution. In the interstellar medium, research suggests that PAHs play a role in unidentified infrared emission bands, diffuse interstellar bands, and the synthesis of precursor molecules to life. To build clean combustion devices and to understand the astrochemical evolution of the interstellar medium, it will be critical to understand the elementary reaction mechanisms under single collision conditions by which these molecules form in the gas phase.

Until recently, this work had been hampered by the difficulty in preparing a large concentration of phenyl radicals, but the phenyl radical represents one of the most important radical species to trigger PAH formation in high-temperature environments. However, we have developed a method for producing these radical species and have undertaken a systematic experimental investigation. In this Account, we report on the chemical dynamics of the phenyl radical (C_6H_5) reactions with the unsaturated hydrocarbons acetylene (C_2H_2), ethylene (C_2H_4), methylacetylene (CH_3CCH), allene (H_2CCCH_2), propylene (CH_3CHCH_2), and benzene (C_6H_6) utilizing the crossed molecular beams approach. For nonsymmetric reactants such as methylacetylene and propylene, steric effects and the larger cones of acceptance drive the addition of the phenyl radical to the nonsubstituted carbon atom of the hydrocarbon reactant. Reaction intermediates decomposed via atomic hydrogen loss pathways. In the phenyl—propylene system, the longer lifetime of the reaction intermediate yielded a more efficient energy randomization compared with the phenyl—methylacetylene system. Therefore, two reaction channels were open: hydrogen losses from the vinyl and from the methyl groups. All fragmentation pathways involved tight exit transition states. In the range of collision energies investigated, the reactions are dictated by phenyl radical addition—hydrogen atom elimination pathways. We did not observe ring closure processes with the benzene ring.

Our investigations present an important step toward a systematic investigation of phenyl radical reactions under single collision conditions similar to those found in combustion flames and in high-temperature interstellar environments. Future experiments at lower collision energies may enhance the lifetimes of the reaction intermediates, which could open up competing ring closure channels to form bicyclic reaction products.

I. Introduction

During the last decades, polycyclic aromatic hydrocarbons (PAHs) together with their hydrogen-deficient precursor molecules have received considerable attention from the combustion chemistry,[1,2] medical,[3] astrophysics,[4] and astrobiology communities.[5] PAHs, which are also considered to be building blocks in the formation of carbonaceous nanoparticles (soot),[6,7] are often associated with incomplete combustion process-

Published on the Web 12/03/2008 www.pubs.acs.org/acr
10.1021/ar8001365 CCC: $71.50

es.[8] Here, soot is primarily composed of nanometer-sized stacks of perturbed graphitic layers that are oriented concentrically in an onion-like fashion.[9] These layers can be characterized as fused benzene rings and are likely formed via agglomeration of PAHs.[10] Those species are emitted to the atmosphere from natural and anthropogenic sources with an average global emission rate of anthropogenic carbon from fossil fuel combustion as high as 2.4×10^{10} kg per year.[11] Once liberated into the ambient environment, PAHs and soot in respirable size of 10−100 nm can be transferred into the lungs by inhalation and are strongly implicated in the degradation of human health,[12] particularly due to their high carcinogenic risk potential. PAHs and carbonaceous nanoparticles are also serious water pollutants of marine ecosystems and bioaccumulate in the fatty tissue of living organisms.[13] Together with leafy vegetables, where PAHs and soot deposit easily, they have been further linked to soil contamination,[14] food poisoning, liver lesions, and tumor growth. Soot particles with diameters up to 500 nm can be transported to high altitudes and influence the atmospheric chemistry.[15] These particles act as condensation nuclei for water ice, accelerate the degradation of ozone, change the Earth's radiation budget, and could lead ultimately to an increased rate of skin cancer on Earth and possibly to a reduced harvest of crops.[16]

Whereas on Earth PAHs are considered severe pollutants and airborne toxic chemicals, in the interstellar medium with temperatures as low as 10 K, PAH-like species are crucial to understanding the astrochemical and astrobiological evolution of carbon-rich environments like circumstellar envelopes of carbon-rich stars, such as IRC+10216, and planetary nebulae. PAH-like species account for up to 10% of the cosmic carbon budget and have been linked to the unidentified infrared (UIR) emission bands observed in the range of 3−14 μm (3300−700 cm^{-1}).[17] They have been further considered a carrier of the diffuse interstellar bands (DIBs), discrete absorption features superimposed on the interstellar extinction curve ranging from the blue part of the visible (400 nm) to the near-infrared (1.2 μm). It should be noted that besides in the interstellar medium, PAHs have also been found in comets[18] and meteorites[19] and have been suggested to be involved in the formation of precursor molecules relevant to life as we know it.[20] A quantitative understanding of the formation of PAHs and their precursors is therefore essential to developing clean combustion devices and to comprehending the astrochemical evolution of distinct interstellar environments.

But how are PAHs and their hydrogen-deficient precursor molecules formed? Present-day reaction networks mimicking PAH formation in combustion flames and in the interstellar medium agree that the phenyl radical (C_6H_5) in its $^2A_1$ electronic ground state presents the most important transient species to trigger PAH formation. The phenyl radical itself has been scavenged as a methylthioether in flames.[21] Recently, the phenyl radical was also assigned via its ionization potential in sooting hydrocarbon flames utilizing tunable vacuum ultraviolet light from synchrotron sources.[22] These reaction networks concur that phenyl radical reactions with unsaturated hydrocarbon molecules such as (substituted) acetylenes, olefins, and aromatic molecules initiate PAH synthesis via an addition of the radical center of the phenyl radical to the π electronic system of the unsaturated coreactant forming doublet radical intermediates. Theoretical investigations coupled with kinetics studies of these reactions suggested that depending on the temperature and pressure conditions, the intermediates either decompose back to the reactants, fragment predominantly via atomic hydrogen loss pathways, isomerize prior to their decomposition, or are stabilized at higher pressures if the lifetime of the intermediate is longer than the time scale necessary to divert the internal energy of the complexes via a third body collision.[23] The kinetics studies, often conducted utilizing cavity ring down spectroscopy, depict rate constants at temperatures up to 1500 K ranging between 10^{-11} and 10^{-12} cm^3 s^{-1}.[24] These studies show also *activation energies* ranging between 5 and 45 kJ mol^{-1} upon addition of the radical to olefins and alkynes.[37] But despite impressive kinetic data, the reaction products, identification of which is crucial for a detailed chemical modeling of combustion processes and PAH formation in the interstellar medium, were rarely determined. Laboratory data on the reaction products formed in bimolecular collisions of phenyl radicals with unsaturated hydrocarbons were lacking for a long time, predominantly due to the experimental difficulty in preparing a large concentration of phenyl radicals.

Systematic laboratory studies to ascertain the reaction products of phenyl radical reactions with unsaturated hydrocarbons in the gas phase have started only recently with the advance of intense supersonic phenyl radical sources as developed in our laboratory. The crossed molecular beam method presents an efficient experimental technique to supply the nature of the reaction products of phenyl radical reactions. Both combustion and interstellar reaction networks have incorporated a series of bimolecular reactions between radicals, atoms, and closed shell species. Since the chemical evolution of each macroscopic environment can in principle be rationalized by a series of bimolecular collisions between the reactant species, a detailed experimental knowledge of the

elementary processes involved at a fundamental microscopic level is therefore desirable to elucidate the primary reaction products. In this context, laboratory experiments under single collision conditions are imperative to identify the primary reaction products of phenyl radical reactions. Here, in a binary collision involving a phenyl radical and a generalized hydrocarbon molecule (RH), which proceeds via complex formation through a reaction intermediate (reaction 1), a single phenyl radical reacts only with one hydrocarbon molecule. Consequently, any collisional stabilization of the intermediate and even consecutive reactions of the primary products can be eliminated. It should be emphasized that only this requirement assures that the nascent reaction products are probed. Note that in "real" denser environments, three-body collisions may take place if the lifetime of the intermediate is longer than the time between collisions. In this case, the reaction intermediate may also be stabilized or undergoes a successive reaction to more complex hydrocarbon molecules.

$$C_6H_5 + RH \rightarrow [C_6H_5RH]^* \rightarrow C_6H_5R + H \qquad (1)$$

In this Account, we review contemporary developments on crossed molecular beam studies of the reactions of phenyl radicals with the unsaturated hydrocarbons acetylene (C_2H_2), ethylene (C_2H_4), methylacetylene (CH_3CCH), allene (H_2CCCH_2), propylene (CH_3CHCH_2), and benzene (C_6H_6). These hydrocarbons serve as simple prototype molecules with triple (acetylene) and double (ethylene) bonds, as well as monocyclic (benzene) aromatic species. Methylacetylene and allene are chosen as the simplest representatives to investigate how the dynamics and kinetics change from one structural isomer to the other. Methylacetylene and propylene have been selected to see how the dynamics changes if a hydrogen atom in acetylene and ethylene is replaced by a methyl group. Reactions with (partially) deuterated reactants were also conducted to elucidate to what extent potential atomic hydrogen loss pathways originate from the phenyl radical or from the closed shell hydrocarbon reactants.

II. The Crossed Molecular Beam Approach

Since the macroscopic alteration of each environment, ranging from high-temperature combustion flames and circumstellar envelopes of carbon stars (few 1000 K) to low temperature hydrocarbon-rich atmospheres of planets and their moons (70−120 K) and cold molecular clouds (10 K), consists of multiple elementary reactions that are a series of *bimolecular encounters* between atoms, radicals, and molecules, a detailed understanding of the mechanisms involved at the most fundamental, microscopic level is crucial. These are experiments under *single collision conditions* in which particles of one supersonic beam (the phenyl radical reactant) are made to "collide" only with particles of a second beam (the closed shell hydrocarbon coreagent). During the last years, various supersonic sources have been established in our laboratory to generate reactive species via laser ablation [ground-state carbon atoms ($C(^3P_j)$),[25] dicarbon (C_2)[26] and tricarbon molecules (C_3),[27] and ground-state boron ($B(^2P_j)$)[28] and silicon atoms ($Si(^3P_j)$)],[29] coupling laser ablation with reactive carrier gases [generation of cyano ($CN(X^2\Sigma^+)$)[30] and *d1*-ethynyl ($CCD(X^2\Sigma^+)$) radical beams],[31] photolytic sources [vinyl (C_2H_3, X^2A')[32] and propargyl (C_3H_3, X^2B_1)],[33] and pyrolytic sources [allyl (C_3H_5, X^2A_2)[34] and phenyl (C_6H_5, X^2A_1)].[35] The crossed molecular beam technique represents the most versatile approach in the elucidation of the energetics and dynamics of elementary reactions, in particular of atom−radical and of radical−molecule reactions.[36−39] In contrast to bulk experiments, where reactants are mixed, the advantage of this approach is the capability to form the reactants in separate supersonic beams. These features provide an unprecedented approach to observe the consequences of a single collision event, preventing secondary collisions and wall effects. In principle, both reactant beams can be prepared in well-defined quantum states before they cross at a specific collision energy under single collision conditions. The products can be monitored via spectroscopic detection schemes such as laser-induced fluorescence (LIF)[40] or Rydberg tagging,[41] via ion imaging probes,[42,43] or via a quadrupole mass spectrometric detector (QMS) with *universal* electron impact ionization or photoionization coupled to a mass spectrometric device.

Here, the crossed molecular beam method with mass spectrometric detection presents the most versatile technique to study these elementary reactions thus permitting the elucidation of the chemical dynamics and, in the case of polyatomic reactions, the primary products. Only recently, technological improvements in the production of unstable species such as the phenyl radical and vacuum technology have allowed the study of elementary reactions of combustion and astrochemical importance. The experiments reported here were conducted with the crossed molecular beams machine at the University of Hawaii (Figure 1).[44] The apparatus consists of two source chambers at a crossing angle of 90°, a stainless steel scattering chamber, and an ultrahigh-vacuum tight, rotatable, differentially pumped quadrupole mass spectrometric (QMS) detector, which can be pumped down to vacuum in the high 10^{-13} Torr range. In the primary source, a *pulsed* supersonic beam of phenyl radicals was generated by flash pyroly-

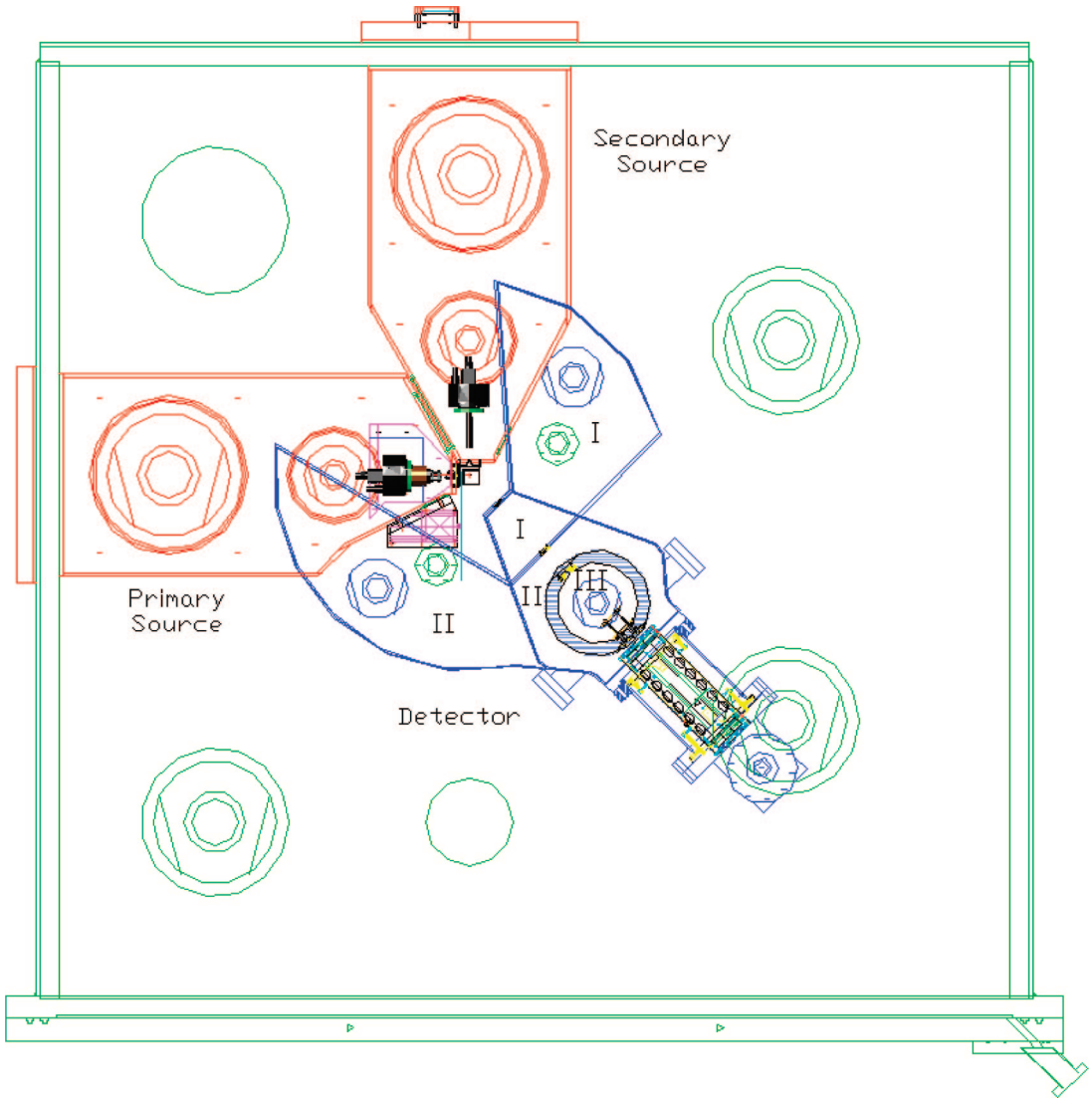

FIGURE 1. Top view of the crossed molecular beams machine depicting the primary source chamber (phenyl radical source), the secondary source chamber (hydrocarbon source), and the triply differentially pumped detector with electron impact ionizer and quadrupole mass spectrometer. Differentially pumped regions are indicated by I, II, and III.

sis of nitrosobenzene (C_6H_5NO) at seeding fractions of less than 0.1% in helium carrier gas employing a modified Chen source[45] coupled to a piezoelectric pulsed valve. With use of helium as a calibration gas, the temperature of the tube was estimated to be around 1200−1500 K. At these experimental conditions, the decomposition of the nitrosobenzene molecule to form nitrogen monoxide and the phenyl radical is quantitative; this means that in the supersonic beam, only nitrogen monoxide, helium, and the phenyl radical exist. The phenyl radical beam is passed through a skimmer into the main chamber; a chopper wheel located after the skimmer and prior to the collision center selects a slice of molecules with well-defined velocity, which reach the interaction region. The phenyl radical beam intersects *pulsed* hydrocarbon beams released by a second pulsed valve under well-defined collision energies ranging from 80 to 185 kJ mol^{-1}. It is important to stress that the incorporation of *pulsed beams* allows reactions with often expensive (partially) deuterated chemicals to be carried out to extract additional information on the reaction dynamics, such as the position of the hydrogen or deuterium loss if multiple reaction pathways are involved.

To detect the product(s), our machine incorporates a triply differentially pumped, *universal* quadrupole mass spectrometric detector coupled to an electron impact ionizer. Here, any reactively scattered species from the collision center after a single collision event has taken place can be ionized in the electron impact ionizer, and in principle, it is possible to determine the mass (and the gross formula) of all the products of

a bimolecular reaction by varying the mass-to-charge ratio, m/z, in the mass filter. Since the detector is rotatable within the plane defined by both beams, this detector makes it possible to map out the angular (LAB) and velocity distributions of the scattered products. Measuring the time-of-flight (TOF) of the products from the interaction region over a finite flight distance at different laboratory angles allows extraction of the product translational energy and angular distributions in the center-of-mass reference frame. This provides insight into the nature of the chemical reaction (direct vs indirect), intermediates involved, the reaction product(s), their branching ratios, and in some cases the preferential rotational axis of the fragmenting complex(es) and the disposal of excess energy into the products' internal degrees of freedom as a function of scattering angle and collision energy. Despite the triply differential pumping setup of the detector chambers, molecules desorbing from wall surfaces lying on a straight line to the electron impact ionizer cannot be avoided. Their mean free path is on the order of 10^3 m compared with maximum dimensions of the detector chamber of about 1 m. To reduce this background, a copper plate attached to a two-stage closed cycle helium refrigerator is placed right before the collision center and cooled to 4 K. In this way, the ionizer views a cooled surface, which traps all species with the exception of hydrogen and helium.

What information can we obtain from these measurements? The observables contain some basic information.[46] Every species can be ionized at the typical electron energy used in the ionizer and, therefore, it is possible to determine the mass and the gross formula of all the possible species produced from the reactions by simply selecting different m/z in the quadrupole mass spectrometer. Even though some problems such as dissociative ionization and background noise limit the method, the advantages with respect to spectroscopic techniques are obvious, since the applicability of the latter needs as a prerequisite the knowledge of the optical properties of the products. Another important aspect is that, by measuring the product velocity distributions, one can immediately derive the amount of the total energy available to the products and, therefore, the enthalpy of reaction of the reactive collision. This is of great help when different structural isomers with different enthalpies of formation can be produced. For a more detailed physical interpretation of the reaction mechanism, it is necessary to transform the laboratory (LAB) data into the center-of-mass (CM) system using a forward-convolution routine.[47] This approach initially assumed an angular distribution, $T(\theta)$, and a translational energy distribution, $P(E_T)$, in the center-of-mass reference frame (CM). TOF spectra and the laboratory angular distribution were then calculated from these center-of-mass functions. The essential output of this process is the generation of a product flux contour map, $I(\theta,u) = P(u)T(\theta)$. This function reports the flux of the reactively scattered products (I) as a function of the center-of-mass scattering angle (θ) and product velocity (u) and is called the reactive *differential cross section*. This map can be seen as the *image* of the chemical reaction and contains *all* the information on the scattering process.

III. Results and Discussion

Here, we review the results of our crossed molecular beam experiments of phenyl radicals with acetylene (C_2H_2), ethylene (C_2H_4), methylacetylene (CH_3CCH), allene (H_2CCCH_2), propylene (CH_3CHCH_2), and benzene (C_6H_6). Specific details and the methodology of this approach are given for the reactions of phenyl radicals with acetylene, ethylene, and benzene. Hereafter, these findings are transferred to the methylacetylene, allene, and propylene reactants. This approach will help us to elucidate generalized concepts on the chemical dynamics and the underlying reaction mechanisms of the reactions of phenyl radicals with unsaturated hydrocarbons in extreme environments and their role in the formation of PAHs and their hydrogen-deficient precursor molecules.

The Reactions of Phenyl Radicals with Acetylene (C_2H_2), Ethylene (C_2H_4), and Benzene (C_6D_6). Reactive scattering signal was detected at mass-to-charge ratios (m/z) of $m/z = 102$ ($C_8H_6^+$) [acetylene],[33] $m/z = 104$ ($C_8H_8^+$) [ethylene],[48] and $m/z = 159$ ($C_{12}H_5D_5^+$) [benzene-d_6][49] (Figure 2a). For all three systems, ion counts were also detected at lower mass to charge ratios. However, at all angles, the TOF spectra monitored at lower m/z values are superimposable to the TOFs taken at $m/z = 102$, 104, and 159 in the acetylene, ethylene, and benzene-d_6 systems. These findings indicate that the phenyl radical reacts with the unsaturated hydrocarbon molecule under elimination of a hydrogen atom (acetylene/ethylene) or a deuterium atom (benzene-d_6) to form hydrocarbon molecules of the gross formulas C_8H_6 [acetylene], C_8H_8 [ethylene], and $C_{12}H_5D_5$ [benzene-d_6]. Furthermore, signal at lower m/z values originate from dissociative ionization of the reaction products in the electron impact ionizer. Note that these data alone do not allow us to elucidate the nature of the product isomer formed. The corresponding laboratory angular distributions are shown in Figure 2b. It should be stressed that in the case of the acetylene and ethylene reactions, the hydrogen atom can be lost from either the phenyl radical or the closed shell molecule. To pin down the position of the

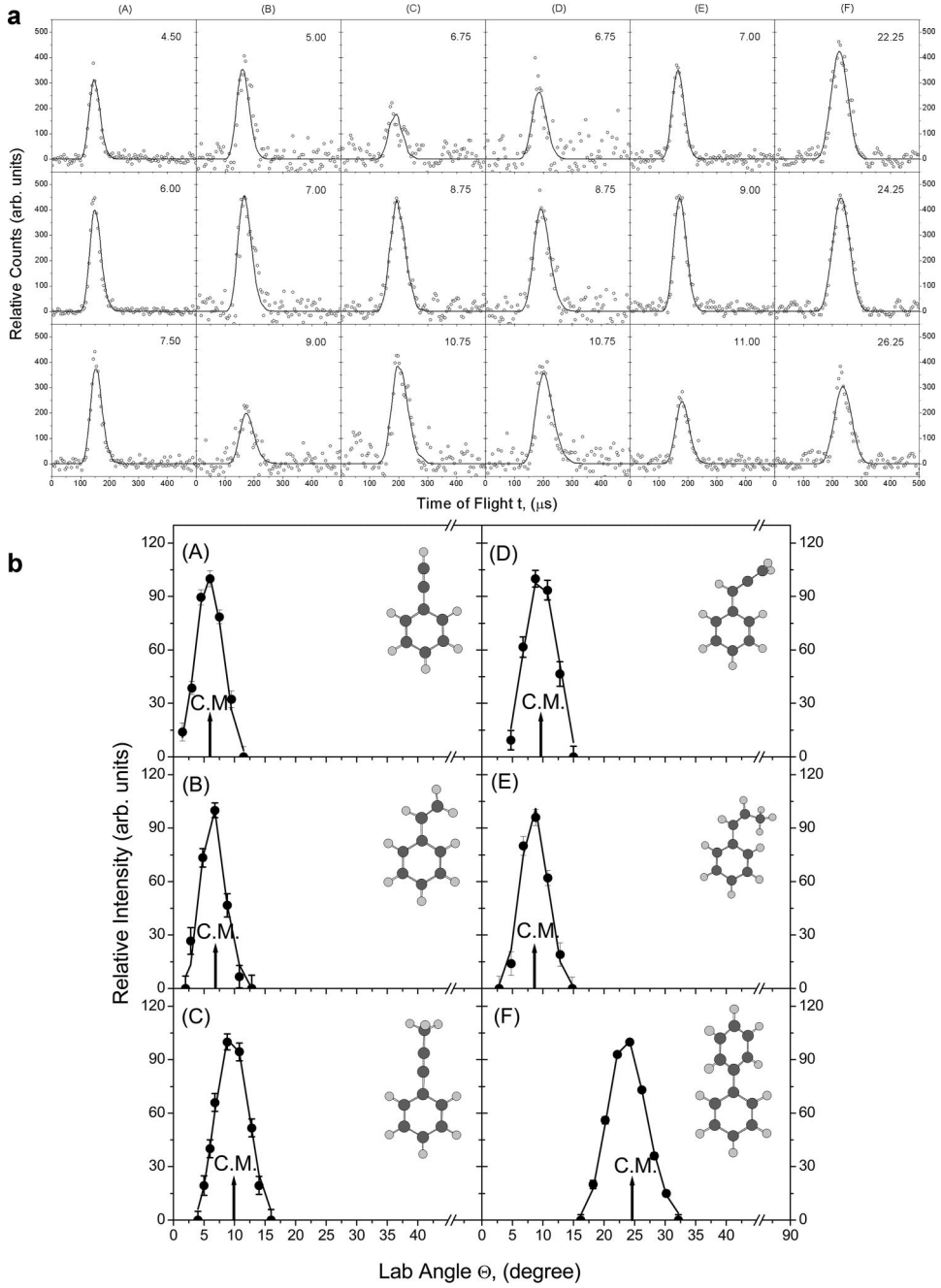

FIGURE 2. (a) Time-of-flight (TOF) spectra of ion counts at mass-to-charge rations (m/z) of 102 ($C_8H_6^+$; A), 104 ($C_8H_8^+$; B), 116 ($C_9H_8^+$; C, D), 118 ($C_9H_{10}^+$; E), and 159 ($C_{12}H_5D_5^+$; F) recorded in the reactions of phenyl radicals with acetylene (A; 99.0 kJ mol^{-1}), ethylene (B; 83.6 kJ mol^{-1}), methylacetylene (C; 91.4 kJ mol^{-1}), allene (D; 92.7 kJ mol^{-1}), propylene (E; 130.2 kJ mol^{-1}), and benzene-d_6 (F; 185.0 kJ mol^{-1}). The collision energies are given in parentheses. (b) Laboratory angular distributions (LAB) of ion counts at mass-to-charge rations (m/z) of 102 ($C_8H_6^+$; A), 104 ($C_8H_8^+$; B), 116 ($C_9H_8^+$; C, D), 118 ($C_9H_{10}^+$; E), and 159 ($C_{12}H_5D_5^+$; F), recorded in the reactions of phenyl radicals with acetylene (A; 99.0 kJ mol^{-1}), ethylene (B; 83.6 kJ mol^{-1}), methylacetylene (C; 91.4 kJ mol^{-1}), allene (D; 92.7 kJ mol^{-1}), propylene (E; 130.2 kJ mol^{-1}), and benzene-d_6 (F; 185.0 kJ mol^{-1}). The arrows indicate the corresponding center-of-mass angles. The circles represent the experimental data and the solid lines the best fits with the center of mass functions shown in Figure 3.

atomic hydrogen loss, we conducted the crossed beam reactions of phenyl radicals with perdeuterated acetylene (C_2D_2) and ethylene (C_2D_4). For instance, for the acetylene-d_2 reactant, the emission of a hydrogen atom from the phenyl group should result in signal at $m/z = 104$ ($C_8H_4D_2^+$); on the other hand, the release of atomic deuterium is expected to be monitored at $m/z = 103$ ($C_8H_5D^+$). An analysis of the data taken demonstrated unequivocally that only deuterium atom losses are observed from acetylene-d_2 and ethylene-d_4. This strongly indicates that under single collision conditions, the phenyl

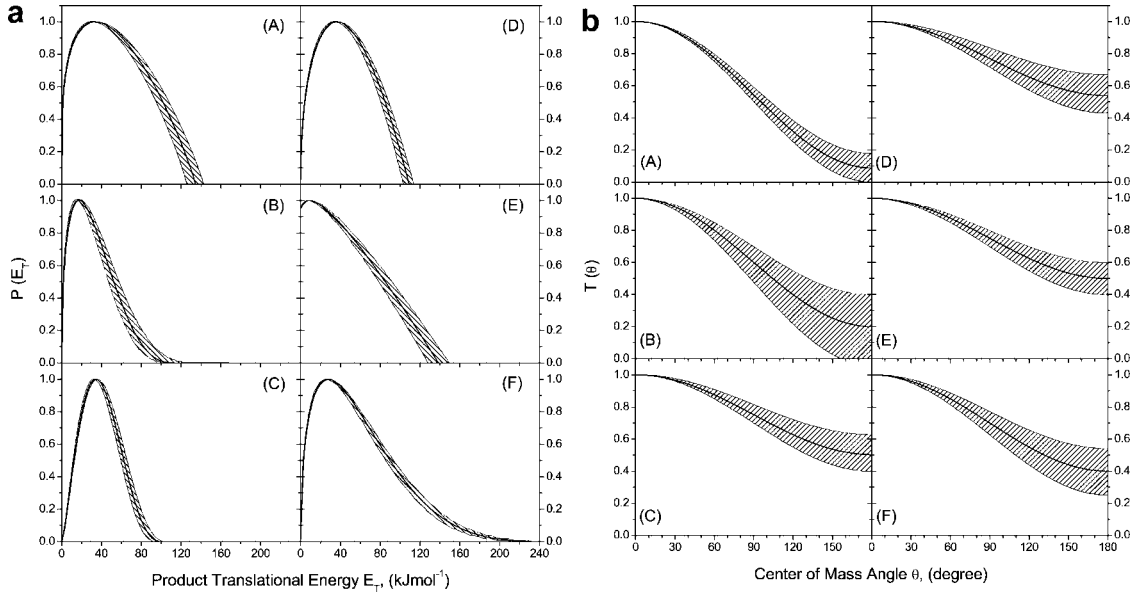

FIGURE 3. Corresponding center-of-mass translational energy distributions (a) and angular distributions (3) extracted from the laboratory data as presented in Figure 2. The solid lines are the best fits, and the hatched areas the acceptable fits within the error limits of the experiments.

group stays intact during the reactions and that the phenyl radical versus deuterium atom replacement pathways are the dominating exit channels for the reactions with perdeuterated acetylene, ethylene, and benzene. These ion counts of the parent ions can be integrated for each system at different angles to obtain the corresponding laboratory angular distributions. As evident from the data, the LAB distributions are very narrow and show a slight asymmetry with a preferred intensity in the forward direction (0°), that is, the direction of the phenyl radical beam.

To collect meaningful information on the chemical dynamics, we must have a detailed look at the derived center-of-mass functions and flux contour maps, which are reported in Figures 3 and 4, respectively. The best fit translational energy distributions, $P(E_T)$ (Figure 3a), are illustrated by characteristic maxima of the translational energy, $E_{T,max}$, of 125−140 (acetylene), 100−120 (ethylene), and 210−230 kJ mol^{-1} (benzene-d_6) reactions. Based on energy conservation, each high-energy cutoff, that is, the maximum translational energy assuming no energy channels into the internal degrees of freedom, represents the sum of the collision energy plus the reaction exoergicity. Therefore, if we subtract the collision energies from these high-energy cutoffs, the phenyl versus hydrogen/deuterium atom exchange pathways are found to be exoergic by 45 ± 11 kJ mol^{-1} (acetylene), 25 ± 12 kJ mol^{-1} (ethylene), and 35 ± 15 kJ mol^{-1} (benzene-d_6). These reaction energies are important to elucidate the nature of the structural isomer formed. We can compare the experimentally determined reaction energies with those obtained from electronic structure calculations or those extracted from the NIST database.[50] This analysis leads us to the conclusion that in the reactions of phenyl radicals with acetylene, ethylene, and benzene-d_6, the nascent reaction products are phenylacetylene (C_6H_5CCH), styrene ($C_6H_5C_2H_3$), and diphenyl-d_5 ($C_6H_5C_6D_5$), respectively. Another important piece of information that can be derived from the translational energy distributions originates from the distribution maxima of the $P(E_T)$s. Here, all distributions were found to peak away from zero translational energy at a range of 15−40 kJ mol^{-1}. These findings might indicate the existence of *exit barriers* when the hydrogen or deuterium atoms are emitted. In other words, the corresponding reversed reactions of hydrogen or deuterium additions to the closed shell hydrocarbon molecule are expected to have *entrance barriers* of this order of magnitude.[51]

Having analyzed the translational energy distributions, we are turning our attention now to the corresponding center-of-mass angular distributions, $T(\theta)$s (Figure 3b) and the angular part of the flux contour plots (Figure 4). For all three systems, best fits could be derived with center-of-mass angular distributions showing intensity over the complete angular range from 0° to 180°. This finding strongly indicates that the reactions of the phenyl radicals with acetylene, ethylene, and benzene-d_6 follow indirect scattering dynamics. This means that the reactions involve the formation of $C_2H_2C_6H_5$, $C_2H_4C_6H_5$, and $C_6D_6C_6H_5$ reaction intermediates. Since we are conducting the reactions under single collision conditions, the absence of wall effects and third body stabilization of these interme-

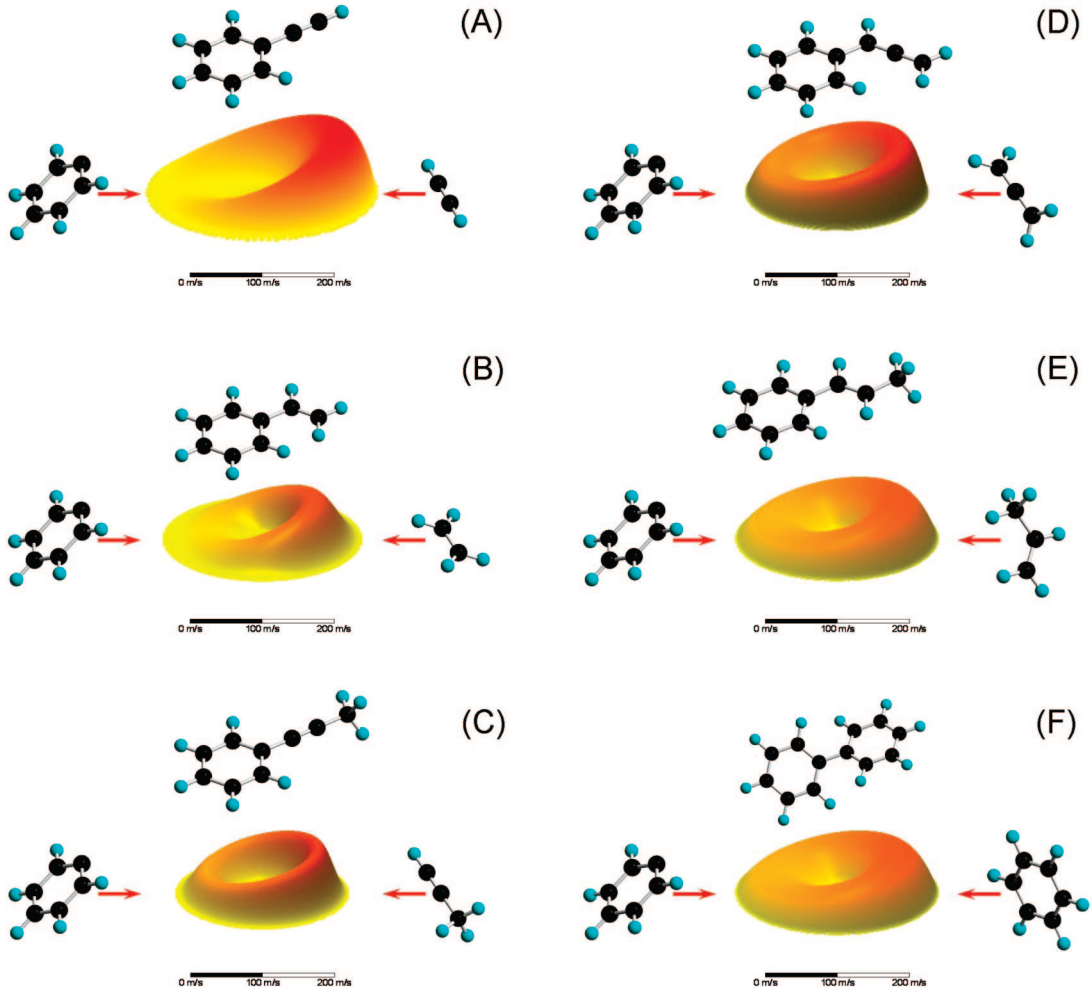

FIGURE 4. Center-of-mass velocity contour flux map for the reaction of phenyl radicals (left, 0°) with six hydrocarbon molecules: acetylene (A), ethylene (B), methylacetylene (C), allene (D), propylene (E), and benzene-d_6 (F) (right, 180°) to form phenylacetylene (A), styrene (B), 1-phenylmethylacetylene (C), phenylallene (D), 1- and 3-phenylpropylene (E), and diphenyl (F). The colors connect data points with an identical flux and range from red (highest flux) to yellow (lowest flux). The units of axis are given in m s^{-1} (see legend).

diates dictates that *all* intermediates are unstable and, hence, fragment due to the high internal energy content (rovibrational excitation of the intermediates). It is important to highlight that the $T(\theta)$s are not symmetric with respect to 90° but show a higher flux in the forward (with respect to the phenyl radical beam) direction compared with the backward direction (closed shell hydrocarbon reactant). These findings strongly indicate that the lifetime of each reaction intermediate is shorter than their rotation periods (osculating complex behavior).[52]

How do our experimental results compare with recent electronic structure calculations on these systems? The relevant parts of the potential energy surfaces (PESs) are compiled in Figure 5. Here, the experimental findings correlate very well with the ab initio calculations. As also suggested by the experimental results, the phenyl radical with its unpaired electron located in a A_1 symmetric σ-like orbital adds via small entrance barriers to the π cloud of acetylene, ethylene, and benzene to form doublet radical intermediates $C_2H_2C_6H_5$,[33] $C_2H_4C_6H_5$,[46] and $C_6D_6C_6H_5$,[47] respectively. It is important to note that crossed molecular beam experiments can predict the existence of these intermediates based on the shape of the center-of-mass angular distributions; however, the experiments could not pin down the energetics of these collision complexes. Here, the electronic structure calculations suggested that all three collision complexes rise in potential energy wells located about 100−170 kJ mol^{-1} below the energy of the separated reactants. These radical intermediates fragment via atomic hydrogen (acetylene, ethylene) and deuterium (benzene-d_6) pathways to form closed shell hydrocarbons phenylacetylene (C_6H_5CCH), styrene ($C_6H_5C_2H_3$), and diphenyl-d_5 ($C_6H_5C_6D_5$). The experimentally derived reaction energies of -45 ± 11 kJ mol^{-1} (acetylene), -25 ± 12 kJ mol^{-1} (ethylene), and -35 ± 15 kJ mol^{-1} (benzene-d_6) agree

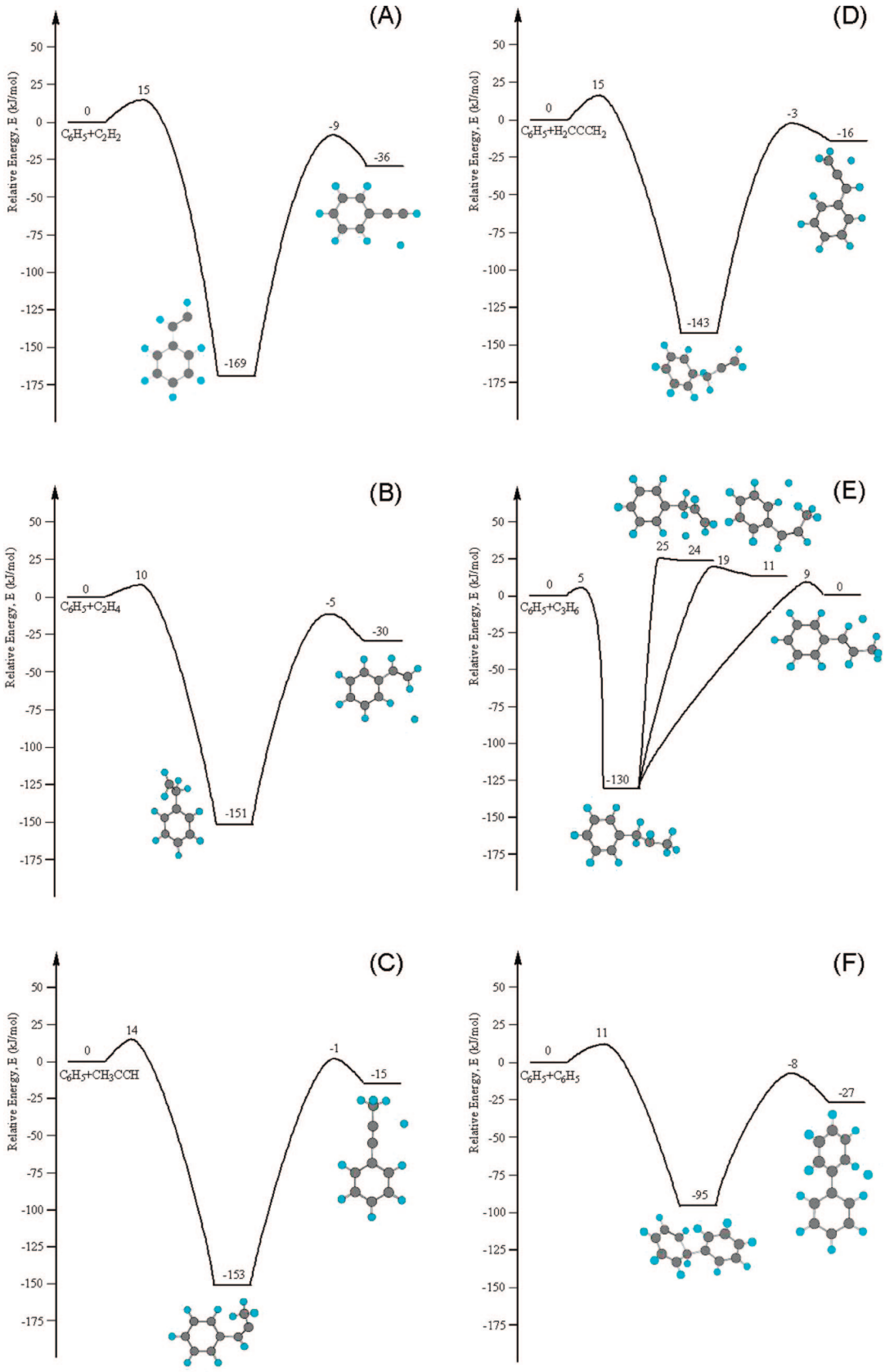

FIGURE 5. Schematic potential energy surfaces for the reactions of phenyl radicals with acetylene (A), ethylene (B), methylacetylene (C), allene (D), propylene (E), and benzene-d_6 (F) to form phenylacetylene (A), styrene (B), 1-phenylmethylacetylene (C), phenylallene (D), 1- and 3-phenylpropylene (E), and diphenyl (F).

nicely with those obtained from electronic structures calculations: -41 ± 8 kJ mol^{-1}, -21 ± 3 kJ mol^{-1}, and -22 ± 8 kJ mol^{-1}, respectively. In addition, the computed exit barriers are confirmed by our experiments and the off-zero peaking of the center-of-mass translational energy distributions.

The Reactions of Phenyl Radicals with Methylacetylene (CH_3CCH), Allene (C_3H_4), and Propylene (CH_3CHCH_2). The reactions of phenyl radicals with methylacetylene and propylene depict important similarities compared with the nonsubstituted acetylene and ethylene reactants but also striking differences. First of all, the experiments verified explicitly that in reactions of phenyl radicals with perdeuterated methylacetylene,[53] propylene,[54] and allene,[51] only a deuterium atom was emitted; no evidence of an atomic hydrogen loss was monitored. This underlined the conclusions extracted from the acetylene, ethylene, and benzene systems that the phenyl group is conserved during the reactions under single collision conditions, at least in the range of collision energies investigated here. However, the methylacetylene and propylene reactants are more complex than the nonsubstituted counterparts and depict nonequivalent hydrogen atoms at the acetylenic and methyl group (methylacetylene) and at the vinyl and methyl group (propylene). Therefore, even the detection of scattering signal at $m/z = 116$ ($C_9H_8^+$; methylacetylene and allene reactants) and $m/z = 118$ ($C_9H_{10}^+$; propylene reactant) makes it difficult to elucidate whether the hydrogen atoms are lost from the methyl group, the acetylenic/vinyl units, or both positions. In these cases, it is very useful to conduct experiments with partially deuterated reactants methylacetylene-d_3 (CD_3CCH) and (propylene-d_3)s ($CD_3C_2H_3$, $CH_3C_2D_3$). Here, the experiments proved explicitly that in the case of the methylacetylene-d_3 reaction, only a hydrogen atom loss (from the acetylenic group) was observed; however, in the case of both propylene-d_3 reactants, the crossed beam studied depicted explicitly hydrogen atom losses from the methyl group ($CH_3C_2D_3$) and from the vinyl group ($CD_3C_2H_3$). Based on the center-of-mass functions and the electronic structure calculations, the following reaction dynamics could be extracted. In case of the phenyl−methylacetylene system, the phenyl radical once again attacks the carbon−carbon triple bond (similar to the acetylene reactant); however, the steric effect and larger cone of acceptance (the methyl group screens the β carbon atom and makes it less accessible to addition) direct the addition process of the radical center of the phenyl radical to the α carbon atom of methylacetylene (the carbon atom holding the acetylenic hydrogen atom). This again leads to indirect scattering dynamics as evident from the center-of-mass angular distribution and also from the bound doublet $C_6H_5HCCCH_3$ intermediate found in the electronic structure calculations. Based on the observed hydrogen loss in the reaction with methylacetylene-d_3 and the energetics of the reaction, this intermediate loses a hydrogen atom from the acetylenic group to form a 1-phenylmethylacetylene molecule ($C_6H_5CCCH_3$) via a small exit barrier. The presence of an exit barrier is also evident from the shape of the center-of-mass translational energy distribution, that is, a peaking of the latter away from zero translational energy. However, a comparison of the phenyl−acetylene and phenyl−methylacetylene system shows a striking difference. An inspection of the pertinent center-of-mass angular distributions extracted from both reactions (Figure 3b) shows a less forward-pronounced distribution in the phenyl−methylacetylene system. This suggest that at comparable collision energies as investigated here the lifetime of the $C_6H_5HCCCH_3$ intermediate is longer compared with the C_6H_5HCCH collision complex formed in the reaction of phenyl radicals with acetylene. On the other hand, the experiments with methylacetylene-d_3 suggested that the lifetime of the $C_6H_5HCCCH_3$ radical is still too low to allow energy randomization to occur so that a deuterium atom could be ejected from the methyl-d_3 group. Note that the chemical dynamics of the phenyl−allene system are similar to those of the methylacetylene isomer. Here, the phenyl radical adds to the terminal carbon atom holding the CH_2 group. The resulting intermediate also ejects atomic hydrogen via a tight exit transition state leading to a phenylallene reaction product ($C_6H_5HCCCH_2$).

Finally, it is interesting to compare the chemical dynamics of the phenyl−propylene system with those of the nonsubstituted reactant (ethylene) but also with the dynamics extracted from the phenyl−methylacetylene system. Similar to the methylacetylene reactant, the phenyl radical adds with its radical center to the nonsubstituted (α carbon) site of the propylene reactant yielding a doublet $C_6H_5CH_2CH(CH_3)$ radical intermediate. The experiments with both (propylene-d_3)s indicated two competing decomposition pathways: a hydrogen atom loss from the methyl group (25%) and also from the vinyl group (75%) leading to at least two distinct isomers via atomic hydrogen atom emission, 3-phenylpropene [$H_2CCH-CH_2C_6H_5$] and *cis*/*trans*-1-phenylpropene [$CH_3CHCHC_6H_5$]. Compared with the methylacetylene reaction, the explicit identification of two isomers suggest that the energy randomization is more complete in the phenyl−propylene system (most probably due to the enhanced number of internal degrees of freedom of the reaction intermediate formed) to allow energy flow from the initially activated bond over the carbon skeleton of the hydrocarbon reactant to the carbon−hydrogen

bond of the methyl group. It is important to highlight that the center-of-mass angular distributions of the phenyl−ethylene system showed explicitly enhanced forward scattering compared with the phenyl−propylene system; this translates into a longer lifetime of the $C_6H_5CH_2CH(CH_3)$ intermediate compared with the $C_6H_5CH_2CH_2$ collision complex; again, this enhanced lifetime is most likely caused by the increased number of internal degrees of freedom in the $C_6H_5CH_2CH(CH_3)$ complex compared with the $C_6H_5CH_2CH_2$ intermediate.

IV. Conclusions and Summary

The dynamics of the phenyl radical (C_6H_5) reactions with unsaturated hydrocarbons acetylene (C_2H_2), ethylene (C_2H_4), methylacetylene (CH_3CCH), allene (H_2CCCH_2), propylene (CH_3CHCH_2), and benzene (C_6H_6) as reported in this Account exposed the reaction intermediates, nascent products of the reactions, exit barriers, and underlying mechanisms. The phenyl radical reactions presented here showed common features. First, the phenyl radical was found to add with its unpaired electron located in its $^2A_1$ orbital to the π electron density of the unsaturated hydrocarbon reactants via indirect scattering dynamics to form reaction intermediates on the doublet potential energy surfaces. In the case of nonsymmetric reactants like methylacetylene and propylene, steric effects and the larger cones of acceptance direct the addition of the phenyl radical to the nonsubstituted carbon atom of the hydrocarbon reactant (α carbon atom). All addition processes have entrance barriers of up to 15 kJ mol^{-1}. Based on this piece of information alone, we must conclude that phenyl radical reactions with unsaturated, closed shell hydrocarbon molecules are closed in the cold regions of the interstellar medium such as in cold molecular clouds where averaged translational temperatures of 10 K reside. Likewise, the low temperatures in the hydrocarbon-rich atmospheres of planets and their satellites such as Titan effectively obstruct these phenyl radical reactions to be efficient in synthesizing precursor molecules to PAHs under low-temperature conditions. Second, as evident from the center-of-mass angular distributions obtained from the reactions with acetylene, ethylene, methylacetylene, and allene, the crossed beam studies depicted nicely that at similar collision energies, the lifetimes of the reaction intermediates increased as the number of internal degrees of freedom of the collision complexes increased. Third, the reaction intermediates were found to decompose via atomic hydrogen loss. In the case of the phenyl−propylene system, the enhanced lifetime of the reaction intermediate allowed a more efficient energy randomization as compared with the phenyl−methylacetylene system; as a consequence, two reaction channels were open: hydrogen losses from the vinyl and from the methyl groups. It should be stressed that reactions of phenyl radicals with perdeuterated reactants verified explicitly that the phenyl group remained intact; only deuterium atom ejection pathways were monitored, but no atomic hydrogen loss was found to be important. Fourth, all fragmentation channels were found to involve tight exit transition states of about 10−25 kJ mol^{-1}. This means that in the reverse reactions of a hydrogen atom with the corresponding closed shell hydrocarbon molecules, an entrance barrier of this order of magnitude is also expected. Fifth, at least in the range of collision energies investigated in the present experiments, the reactions are dictated by phenyl radical addition−hydrogen atom elimination pathways; no ring closure processes with the benzene ring were found to proceed to completion. However, reactions at lower collision energies, which will be investigated in the near future, will certainly lead to enhanced lifetimes of the reaction intermediates. This could also result in competing ring closure channels, which in turn should lead to observable deuterium atom elimination products in case of reactions of phenyl radicals with perdeuterated hydrocarbon reactants. Sixth, besides the closed shell reaction products, we have identified various radical intermediates. These structures could be stabilized or undergo subsequent reactions in high-density combustion flames if the lifetime of the reaction intermediates is longer than the time between collisions.

In summary, we have presented reaction mechanisms and information on the chemical dynamics of reactions of phenyl radicals with unsaturated hydrocarbon molecules. These investigations present an important step toward a systematic investigation of phenyl radical reactions under single collision conditions and help to unravel the underlying organic chemistry to form polycyclic aromatic hydrocarbon molecules and their precursors in high-temperature combustion flames and in circumstellar envelopes of carbon stars, as well as planetary nebulae. A combination of the rate constants obtained from kinetic studies with the nascent reaction products should expose the role of this reaction class to form PAHs and related compounds in combustion systems and high-temperature extraterrestrial environments. In the coming years, future experiments under single collision conditions should be also conducted at lower collision energies; this may enhance the lifetime of the collision complexes and could also lead to competing ring-closure processes finally yielding bicyclic PAH-like structures. Likewise, reactions of phenyl radicals with complex hydrocarbons such as C_4H_6 isomers 1,3-butadiene are

expected to yield unprecedented information of the role of this reaction class in the stepwise build-up of naphthalene molecules and their acyclic isomers in combustion systems and in the hotter regions of the interstellar medium.

This work was supported by the US Department of Energy, Basic Energy Sciences (Grant DE-FG02-03ER15411). We would like to thank Prof. Nadia Balucani, University of Perugia, for comments on this manuscript.

Note Added after ASAP. This paper was posted to the web on December 3, 2008 with an error in the section: The Reactions of Phenyl Radicals with Acetylene (C_2H_2), Ethylene (C_2H_4), and Benzene (C_6D_6). The revised version was posted on January 28, 2009.

BIOGRAPHICAL INFORMATION

Xibin Gu (born in 1973) obtained his Ph.D. in Chemistry from the Dalian Institute of Chemical Physics (China) in 2003. He joined the University of Hawaii at Manoa, Department of Chemistry, as a postdoctoral fellow in 2003 to conduct crossed molecular beam experiments on the dynamics and energetics of reactive intermediates relevant to the chemistry of combustion flames. In 2006, he was appointed Junior Researcher at The University of Hawaii.

Ralf I. Kaiser (born in 1966) received his Ph.D. in Chemistry from the University of Münster (Germany) and Nuclear Research Center (Jülich) in 1994. He conducted postdoctoral work on the gas phase formation of combustion-relevant and astrophysically important molecules at UC Berkeley (Department of Chemistry). From 1997 to 2000, he received a fellowship from the German Research Council (DFG) to perform his *Habilitation* at the Department of Physics (University of Chemnitz, Germany) and Institute of Atomic and Molecular Sciences (Academia Sinica, Taiwan). After a brief stay at the Department of Chemistry, University of York (U.K.), he joined the Department of Chemistry at the University of Hawaii at Manoa in 2002 where he is currently a Professor of Chemistry.

REFERENCES

1 Combustion Chemistry: Elementary Reactions to Macroscopic Processes. *Faraday Discuss.* **2001**, *119*, 1−475.

2 Nienow, A. M.; Roberts, J. T. Heterogeneous chemistry of carbon aerosols. *Annu. Rev. Phys. Chem.* **2006**, *57*, 105–128.

3 Burchiel, S. W.; Luster, M. I. Signaling by environmental polycyclic aromatic hydrocarbons in human lymphocytes. *Clin. Immunol.* **2001**, *98*, 2–10.

4 Duley, W. W. Polycyclic aromatic hydrocarbons, carbon nanoparticles and the diffuse interstellar bands. *Faraday Discuss.* **2006**, *133*, 415–425.

5 Ehrenfreund, P.; Sephton, M. A. Carbon molecules in space: From astrochemistry to astrobiology. *Faraday Discuss.* **2006**, *133*, 277–288.

6 Kroto, H. A postbuckminsterfullerene view of carbon in the galaxy. *Acc. Chem. Res.* **1992**, *25*, 106–112.

7 Kroto, H. Space, stars, C_{60}, and soot. *Science* **1988**, *242*, 1139–1145.

8 Ergut, A.; Levendis, Y. A.; Richter, H.; Carlson, J. , Investigation of soot onset threshold in one-dimensional, laminar, atmospheric pressure, premixed, ethylbenzene flames. Presented at the Fourth Joint Meeting of the U.S. Sections of the Combustion Institute, 2005.

9 Stanmore, B. R.; Brilhac, J. F.; Gilot, P. The oxidation of soot: A review of experiments, mechanisms, and models. *Carbon* **2001**, *39*, 2247–2268.

10 Baird, C. *Environmental Chemistry*; W H. Freeman Company: New York, 1999.

11 Aubin, D. G.; Abbatt, J. P. Adsorption of gas phase nitric acid to n-hexane soot: Thermodynamics and mechanisms. *J. Phys. Chem. A* **2003**, *107*, 11030–11037.

12 Sabin, L. D.; Kozawa, K.; Behrentz, E.; Winer, A. M.; Fitz, D. R.; Pankratz, D. V.; Colome, S. D.; Fruin, S. A. Analysis of real-time variables affecting children's exposure to diesel-related pollutants during school bus commutes in Los Angeles. *Atmos. Environ.* **2005**, *39*, 5243–5254.

13 Hylland, K. Polycyclic aromatic hydrocarbon (PAH) ecotoxicology in marine ecosystems. *J. Toxicol. Environ. Health, Part A* **2006**, *69*, 109–123.

14 Oleszczuk, P.; Baran, S. Influence of soil fertilization by sewage sludge on the content of polycyclic aromatic hydrocarbons (PAHs) in crops. *J. Environ. Sci. Health, Part A* **2005**, *40*, 2085–2103.

15 Wayne, R. P. *Chemistry of the Atmosphere*; Oxford University Press: Oxford, U.K., 2000.

16 Smith, D. M.; Chughtai, A. R. Photochemical effects in the heterogeneous reaction of soot with ozone at low concentrations. *J. Atmos. Chem.* **1997**, *26*, 77–91.

17 Pendleton, Y. J.; Allamandola, L. J. The organic refractory material in the diffuse interstellar medium: Mid-infrared spectroscopic constraints. *Astrophys. J., Suppl. Ser.* **2002**, *138*, 75–98.

18 Clairemidi, J.; Brechignac, P.; Moreels, G.; Pautet, D. Tentative identification of pyrene as a polycyclic aromatic molecule in UV spectra of comet P/Halley: An emission from 368 to 384 nm. *Planet. Space Sci.* **2004**, *52*, 761–772.

19 Stephan, T.; Jessberger, E. K.; Heiss, C. H.; Rost, D. TOF-SIMS analysis of polycyclic aromatic hydrocarbons in Allan Hills 84001. *Meteorit. Planet. Sci.* **2003**, *38*, 109–116.

20 Botta, O. Organic Chemistry in Meteorites, Comets, and the Interstellar Medium. In *Astrochemistry: Recent Successes and Current Challenges, Proceedings of the 231st Symposium of the International Astronomical Union*; Lis, D. C., Blake, G. A., Herbst, E., Eds. Cambridge University Press: Cambridge, U.K., 2005; pp 479−488.

21 Hausmann, M.; Homann, K. H. Radical analysis in flames by scavenging with dimethyl disulfide. Presented at the 22nd International Annual Conference of ICT, 1991 (Combustion and Reaction Kinetics),22/1−12.

22 Law, M. E.; Westmoreland, P. R.; Cool, T. A.; Wang, J.; Hansen, N.; Taatjes, C. A.; Kasper, T. Benzene precursors and formation routes in a stoichiometric cyclohexane flame. *Proc. Combust. Inst.* **2007**, *31*, 565–573.

23 Park, J.; Tokmakov, I. V.; Lin, M. C. Experimental and computational studies of the phenyl radical reaction with allene. *J. Phys. Chem. A* **2007**, *111*, 6881–6889.

24 Tokmakov, I. V.; Lin, M. C. Combined quantum chemical/RRKM-ME computational study of the phenyl + ethylene, vinyl + benzene, and H + styrene reactions. *J. Phys. Chem. A* **2004**, *108*, 9697–9714. Fahr, A.; Stein, S. E. Reactions of vinyl and phenyl radicals with ethyne, ethene and benzene. *Symp. Int. Combust. Proc.* **1989**, *22*, 1023–1029. Tokmakov, I. V.; Park, J.; Lin, M. C. Experimental and computational studies of the phenyl radical reaction with propyne. *ChemPhysChem* **2005**, *6*, 2075–2085. Park, J.; Nam, G. J.; Tokmakov, I. V.; Lin, M. C. Experimental and theoretical studies of the phenyl radical reaction with propene. *J. Phys. Chem. A* **2006**, *110*, 8729–8735.

25 Kaiser, R. I.; Suits, A. G. A high-intensity, pulsed supersonic carbon source with $C(^3P_j)$ kinetic energies of 0.08−0.7 eV for crossed beam experiments. *Rev. Sci. Instrum.* **1995**, *66*, 5405–5411. Kaiser, R. I.; Lee, Y. T.; Suits, A. G. Crossed beam reaction of $C(^3P_j)$ with $C_2H_2(^1\Sigma_g^+)$: Observation of tricarbon-hydride C_3H. *J. Chem. Phys.* **1995**, *103*, 10395–10398.

26 Kaiser, R. I.; Balucani, N.; Charkin, D. O.; Mebel, A. M. A crossed beam and ab initio study of the $C_2 + C_2H_2(X^1\Sigma_g^+)$ reactions. *Chem. Phys. Lett.* **2003**, *382*, 112–119.

27 Guo, Y.; Gu, X.; Zhang, F.; Mebel, A. M.; Kaiser, R. I. A crossed molecular beam study on the formation of hexenediynyl radicals ($H_2CCCCCH$; C_6H_3 (X^2A')) via reactions of tricarbon molecules, $C_3(X^1\Sigma_g^+)$, with Allene (H_2CCCH_2; X^1A_1) and methylacetylene (CH_3CCH; X^1A_1). *Phys. Chem. Chem. Phys.* **2007**, *9*, 1972–1979.

28 Zhang, F.; Guo, Y.; Gu, X.; Kaiser, R. I. A crossed molecular beam study on the reaction of boron atoms, $B(^2P_j)$, with Benzene, C_6H_6 (X^1A_{1g}), and D6−benzene $C_6D_6(X^1A_{1g})$. *Chem. Phys. Lett.* **2007**, *440*, 56–63.

29 Kaiser, R. I. General Discussion. *Faraday Discuss.* **2006**, *133*, 227–247.

30 Huang, L. C. L.; Lee, Y. T.; Kaiser, R. I. Crossed beam reaction of the cyanogen radical, $CN(X^2\Sigma^+)$, with acetylene, $C_2H_2(X^1\Sigma_g^+)$: Observation of cyanoacetylene, HCCCN ($X^1\Sigma^+$). *J. Chem. Phys.* **1999**, *110*, 7119–7122.

31 Kaiser, R. I.; Chiong, C. C.; Asvany, O.; Lee, Y. T.; Stahl, F.; Schleyer, P. v. R.; Schaefer, H. F., III. Chemical dynamics of d1-methyldiacetylene (CH3CCCCD; X^1A_1) and d1-ethynylallene (H2CCCH(C2D); X^1A') formation from reaction of $C_2D(X^2\Sigma^+)$ with methylacetylene $CH_3CCH(X^1A_1)$. *J. Chem. Phys.* **2001**, *114*, 3488–3496.

32 Kaiser, R. I.; Ochsenfeld, C.; Stranges, D.; Head-Gordon, M.; Lee, Y. T. Combined crossed molecular beams and ab initio investigation of the formation of carbon-

bearing molecules in the interstellar medium via neutral-neutral reactions. *Faraday Discuss.* **1998**, *109*, 183–204.

33 Kaiser, R. I.; Sun, W.; Suits, A. G.; Lee, Y. T. Crossed beam reaction of atomic carbon, $C(^3P_j)$, with the propargyl radical, $C_3H_3(X^2B_2)$: Observation of diacetylene, $C_4H_2(X^1\Sigma_g^+)$. *J. Chem. Phys.* **1997**, *107*, 8713–8716.

34 Guo, Y.; Mebel, A. M.; Zhang, F.; Gu, X.; Kaiser, R. I. Crossed molecular beam studies of the reactions of allyl radicals, $C_3H_5(X^2A_2)$ with methylacetylene ($CH_3CCH(X^1A_1)$), allene ($H_2CCCH_2(X^1A_1)$), and their isotopomers. *J. Phys. Chem. A* **2007**, *111*, 4914–4921.

35 Gu, X.; Zhang, F.; Guo, Y.; Kaiser, R. I. A crossed molecular beam study on the formation of phenylacetylene from phenyl radicals and acetylene. *Angew. Chem., Int. Ed.* **2007**, *46*, 6866–6869.

36 Kaiser, R. I. Experimental investigation on the formation of carbon-bearing molecules in the interstellar medium via neutral−neutral reactions. *Chem. Rev.* **2002**, *102*, 1309–1358.

37 Liu, K. Recent advances in crossed-beam studies of bimolecular reactions. *J. Chem. Phys.* **2006**, *125*, 132307.

38 Lee, Y. T. Reactive Scattering I: Nonoptical Methods. In *Atomic and Molecular Beam Methods*; Scoles, G., Ed.; Oxford University Press: Oxford, U.K., 1988.

39 Casavecchia, P.; Capozza, G.; Segoloni, E. Crossed molecular beam reactive scattering: Towards universal product detection by soft electron-impact ionization. In *Modern Trends in Chemical Reaction Dynamics, Part 2*; Yang, X., Liu, K., Eds.; Advanced Series in Physical Chemistry; World Scientific: Singapore, 2004; Vol *14*, pp 329−381.

40 Nam, M. J.; Youn, S. E.; Choi, J. H. A study of the radical−radical dynamics of $O(^3P)$ + t-C_4H_9 → OH + iso-C_4H_8. *J. Chem. Phys.* **2006**, *124*, 104307.

41 Witinski, M. F.; Ortiz-Suarez, M.; Davis, H. F. Reaction dynamics of $CN+O_2 \rightarrow NCO+O(^3P_2)$. *J. Chem. Phys.* **2006**, *124*, 094307.

42 Townsend, D.; Li, W.; Lee, S. K.; Gross, R. L.; Suits, A. G. Universal and state-resolved imaging of chemical dynamics. *J. Phys. Chem. A* **2005**, *109*, 8661–8674.

43 Li, W.; Huang, C.; Patel, M.; Wilson, D; Suits, A. G. State-resolved reactive scattering by slice imaging: A new view of the Cl + C_2H_6 reaction. *J. Chem. Phys.* **2006**, *124*, 011102.

44 Gu, X.; Guo, Y.; Zhang, F.; Mebel, A. M.; Kaiser, R. I. Reaction dynamics of carbon-bearing radicals in circumstellar envelopes of carbon stars. *Faraday Discuss.* **2006**, *133*, 245–275.

45 Kohn, D. W.; Clauberg, H.; Chen, P. Flash pyrolysis nozzle for generation of radicals in a supersonic jet expansion. *Rev. Sci. Instrum.* **1992**, *63*, 4003–4005.

46 Kaiser, R. I.; Balucani, N. The formation of nitriles in hydrocarbon-rich atmospheres of planets and their satellites: Laboratory investigations by the crossed molecular beam technique. *Acc. Chem. Res.* **2001**, *34*, 699–706.

47 Weis, M. S. Ph D. Thesis, University of California, Berkeley, 1986.

48 Zhang, F.; Gu, X.; Guo, Y.; Kaiser, R. I. Reaction dynamics on the formation of styrene ($C_6H_5C_2H_3$)—A crossed molecular beam study of the reaction of phenyl radicals (C_6H_5) with ethylene (C_2H_4). *J. Org. Chem.* **2007**, *72*, 7597–7604.

49 Zhang, F.; Gu, X.; Kaiser, R. I. Formation of the diphenyl molecule in the crossed beam reaction of phenyl radicals with benzene. *J. Chem. Phys.* **2008**, *128*, 084315.

50 http://webbook.nist.gov/chemistry/.

51 Levine, R. D. *Molecular Reaction Dynamics*; Cambridge UniversityPress: Cambridge, U.K., 2005.

52 Miller, W. B.; Safron, S. A.; Herschbach, D. R. Exchange reactions of alkali atoms with alkali halides. Collision complex mechanism. *Discuss. Faraday Soc.* **1967**, *44*, 108–122.

53 Gu, X.; Zhang, F.; Guo, Y.; Kaiser, R. I. Reaction dynamics of phenyl radicals (C_6H_5, X^2A_1) with methylacetylene ($CH_3CCH(X^1A_1)$), allene ($H_2CCCH_2(X^1A_1)$), and their D4-isotopomers. *J. Phys. Chem. A* **2007**, *111*, 11450–11459.

54 Zhang, F.; Gu, X.; Guo, Y.; Kaiser, R. I. Reaction dynamics of phenyl radicals (C_6H_5) with propylene (CH_3CHCH_2) and its deuterated isotopologues. *J. Phys. Chem. A* **2008**, *112*, 3284–3290.